ELSEVIER

Oxygen partial pressure dependence of electrical conductivity in γ'-Bi$_2$MoO$_6$

C.M.C. Vera[a,*], R. Aragón[a,b]

[a]Laboratorio de Películas Delgadas, Facultad de Ingeniería, Universidad de Buenos Aires, Paseo Colón 850, (1063) Buenos Aires, Argentina
[b]CINSO, CONICET, CITEFA, Lasalle 4397,Villa Martelli, Buenos Aires, Argentina

Abstract

The electrical conductivity of γ'-Bi$_2$MoO$_6$ was surveyed between 450 and 750 °C as a function of oxygen partial pressure, in the range 0.01–1 atm. A $-\frac{1}{6}$ power law dependence, consistent with a Frenkel defect model of doubly ionized oxygen vacancies and interstitials, is evidence for an n-type semiconductive component, with an optical band gap of 2.9 eV. The absence of this dependence is used to map the onset of dominant ionic conduction.
© 2008 Elsevier Inc. All rights reserved.

Keywords: Bismuth molybdates; Electrical transport; Oxygen ionic conduction; Photoconductivity

1. Introduction

The orthorhombic oxide γ-Bi$_2$MoO$_6$ is constituted by layers of $[MoO_4^{2-}]_n$ and $[Bi_2O_2]_n^{2+}$ linked by O^{2-}. Three polymorphs have been described: γ below 570 °C, γ'' between 604 and 640 °C, and the high temperature γ' phase into which they transform irreversibly. In the latter, the $[Bi_2O_2]_n^{2+}$ layers reorder conforming rows of channels in a Latin cross configuration, which make fast oxygen transport possible [1,2].

The high mobility of oxygen in the layered γ'-Bi$_2$MoO$_6$ structure mediates its catalytic properties in selective oxidation of organic reagents. Although electrical transport in this phase is generally acknowledged to be a thermally promoted process, considerable disagreement persists on the relevant conduction mechanism, which has been alternatively attributed to n-type semiconduction [3], fast ionic [4] and mixed [5–7] ionic–electronic conduction.

Impedance spectroscopy studies [8] have shown that electrical transport in typical ceramic samples includes, in addition to ionic and electronic components, grain boundary as well as intracrystalline contributions, which can obscure the dependence of electrical conductivity on partial pressure of oxygen, relevant to the underlying point defect structure.

2. Model conduction in MO

The derivation of the pertinent phenomenological relations can be summarized briefly, invoking a simple undoped semiconducting metal monoxide MO, as a model for the pseudobinary approximation, with a Frenkel point defect structure symbolized by the Kröger–Vink [9] notation:

O_O : lattice oxygen
M_M: lattice metal
O_i: interstitial oxygen
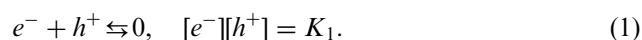M_i: interstitial metal
V_O: oxygen vacancy
V_M: metal vacancy
V_i: interstitial vacancy
$[a]$: concentration of species a

The three pertinent reactions [10,11] and their associated equilibrium expressions are:
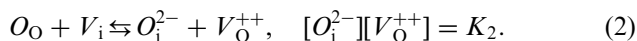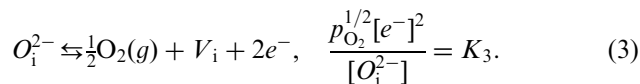
(1) Electron–hole annihilation

$$e^- + h^+ \leftrightarrows 0, \quad [e^-][h^+] = K_1. \tag{1}$$

*Corresponding author.
 E-mail address: cvera@fi.uba.ar (C.M.C. Vera).

(2) Oxygen Frenkel disorder

$$O_O + V_i \leftrightarrows O_i^{2-} + V_O^{++}, \quad [O_i^{2-}][V_O^{++}] = K_2. \qquad (2)$$

(3) Addition or removal of oxygen by interaction with the gas phase

$$O_i^{2-} \leftrightarrows \tfrac{1}{2}O_2(g) + V_i + 2e^-, \quad \frac{p_{O_2}^{1/2}[e^-]^2}{[O_i^{2-}]} = K_3. \qquad (3)$$

Furthermore, preservation of electroneutrality requires that:

$$[e^-] + 2[O_i^{2-}] = [h^+] + 2[V_O^{++}]. \qquad (4)$$

This set of equations admits simple solutions, whenever one species is dominant, which results in four generally recognized limiting cases, namely:

I If ionic defect concentrations are negligible, the concentration of holes is equal to that of electrons, yielding intrinsic semiconductor behavior.

II If electronic carrier concentrations are negligible and the partial pressure of oxygen corresponds to the equilibrium value for the stoichiometric phase, Eq. (4) requires $[O_i^{2-}] = [V_O^{++}]$, corresponding to intrinsic ionic conduction, which is invariant with changes in partial pressure of oxygen.

III In the immediate neighborhood of the stoichiometric composition, consistently with low overall electronic carrier concentrations, their relative changes, induced by reactions 1 and 3, are much larger than those corresponding to ionic defects. Consequently, $[O_i^{2-}]$ and $[V_O^{++}]$ may be presumed constant, yielding the approximation:

$$p_{O_2}^{1/2}[e^-]^2 = K_3[O_i^{2-}], \qquad (5)$$

hence,

$$[e^-] = K_3' p_{O_2}^{-1/4} \qquad (6)$$

and

$$[h^+] = K_3'' p_{O_2}^{1/4}, \qquad (7)$$

where $K_3' = (K_3[O_i^{2-}])^{1/2}$ and $K_3'' = (K_1^2/K_3[O_i^{2-}])^{1/2}$.

IV If the imposed partial pressure of oxygen is significantly lower or higher, than the intrinsic equilibrium value for the stoichiometric oxide, the composition of the solid phase must be alternatively represented by $MO_{1-\delta}$ or $MO_{1+\delta}$, respectively, and the previous approximations are no longer valid, instead it is recognized that:

(a) Far below the intrinsic oxygen partial pressure for the stoichiometric oxide, reaction (3) is favored, which yields high $[e^-]$ and low $[h^+]$. Preservation of electroneutrality requires diminished $[O_i^{2-}]$

and increased $[V_O^{++}]$, consistent with the approximation:

$$[e^-] = 2[V_O^{++}]. \qquad (8)$$

Substitution in (2) and (3) yields

$$[e^-] = K_3^* p_{O_2}^{-1/6}, \qquad (9)$$

where $K_3^* = (2K_2K_3)^{1/3}$.

Far above the intrinsic oxygen partial pressure for the stoichiometric oxide, the reverse holds true, namely low $[e^-]$ and high $[h^+]$. Hence $[O_i^{2-}]$ must increase, whereas $[V_O^{++}]$ decreases, and charge balance requires:

$$[h^+] = 2[O_i^{2-}] \qquad (10)$$

and substitution in (1) and (3) yields

$$[h^+] = K_3^{**} p_{O_2}^{1/6}, \qquad (11)$$

where $K_3^{**} = (2K_1^2/K_3)^{1/3}$.

Alternatives (a) and (b) correspond to mixed ionic–electronic conduction.

3. Mixed ionic–electronic conduction in γ'-Bi$_2$MoO$_6$

Evidence for electronic semiconducting properties can be readily obtained from diffuse optical scattering [12–14] experiments. The spectrum of a sintered pellet (Fig. 1) between 200 and 850 nm, obtained with a Shimadzu Model UV-2401 PC spectrometer, fitted with an integrating sphere, referred to BaSO$_4$ as 100% reflectance standard, displays a characteristic absorption edge around 450 nm, which corresponds to a band gap (E_g) of 2.9 eV, once the linear part of the corresponding Kubelka Munk remission function (inset Fig. 1) is extrapolated. The power law dependence of the absorption coefficient (α) on incident radiation energy ($h\nu$), $\alpha = (h\nu - E_g)^\gamma$, closely fits an exponent $\gamma = \tfrac{1}{2}$, consistent with a direct gap semiconductor [12].
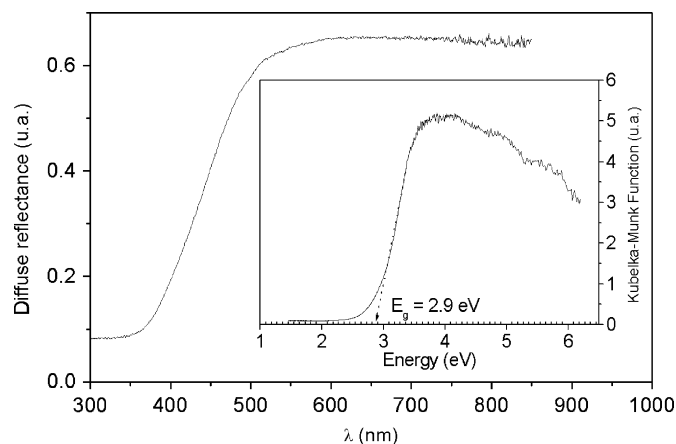

Fig. 1. Diffuse reflectance spectrum of a sintered γ'-Bi$_2$MoO$_6$ pellet, inset: extrapolation to the abscissa of the Kubelka–Munk functional dependence on incident illumination energy yields the semiconductor energy gap.

The electronic contribution to conduction is clearly evidenced by photoexcitation [15]. A Xe lamp pulse, monitored by a photodiode (Fig. 2a) with a Tektronix TDS 220 dual channel oscilloscope, induces a characteristic photocurrent response (Fig. 2b), amplified by a Signal Recovery Model 5182 current preamplifier operated at 10^{-8} A/V, upon incidence on a γ'-Bi_2MoO_6 thick film, heated to 235 °C. No effort was made to fit minority carrier half life, because the shortest light pulse (100 μs) available for this work, is clearly longer than the observed relaxation. Unfortunately, this selective response is not available above the inversion temperature, estimated at 250 °C, because thermally promoted carriers far exceed photoexcited electrons.

Since the activation energy for ionic conduction, obtained from impedance spectroscopy [16] (0.98 eV for grain boundary and 0.73 eV for grain interior conduction), is much smaller than the electronic band gap, a gradual increase in the ionic contribution to overall conduction occurs with increasing temperature. Hence, the classic Wagner experiments to evaluate the relevant transport numbers are inconclusive [17], because at the temperatures required by suitable membrane materials (>600 °C), ionic conduction is dominant in γ'-Bi_2MoO_6 and its small electronic conduction must be evaluated from the difference of two large magnitudes. The alternative explored in this work addresses the characterization of the total electrical conductivity dependence on oxygen partial pressure [18], which can be essentially attributed to electronic processes, as shown above.

4. Experimental

Bi_2MoO_6 was prepared by solid state reaction of reagent grade Bi_2O_3 and MoO_3, ground in stoichiometric propor-tion, pressed into 9×3 mm^2 pellets and sintered at 900 °C in air. The procedure was repeated until XRD confirmed the identity of the γ'-phase and SEM examination established an average 10 μm grain size.

The 100 nm gold electrodes were deposited on both sides of the pellets by magnetron DC sputtering, which were inserted in a spring loaded ceramic fixture, fitted with platinum leads in pseudo four probe configuration and a Platinel II thermocouple, lodged in the air tight cylindrical reactor of a Lindberg Minimite tube furnace. Controlled atmospheres were secured by continuous flow of 100 cm^3/ min of N_2–O_2 mixtures regulated by independent MKS 1179A mass flow controllers.

It was established [19] that ohmic behavior is restricted to voltage drops below 50 mV rms. Due to the strong polarization phenomena associated with ionic conduction, usually minimized by AC excitation, which also provides the benefits of superior noise rejection through lock-in detection. A frequency of 10 Hz was adopted for all measurements as a compromise for a low frequency compatible with reasonable filtering time constants.

A Signal Recovery Model 7265 lock-in amplifier operated in internal mode provided the 50 mV, 10 Hz excitation and demodulated the current signal preamplified by an ad hoc current to voltage converter.

5. Results and discussion

The temporal dependence of conductivity isotherms, monitored at 50 °C intervals between 450 and 750 °C, at constant partial pressures of oxygen between 1 and 0.01 atm (illustrated by a representative data set at 500 °C in Fig. 3), can be extrapolated to obtain estimates of the isothermal equilibrium values as a function of p_{O_2} (Fig. 4a and b), which can be fitted to the functional dependence:

$$\log \sigma = K + N \log p_{O_2} \qquad (12)$$

derived by substitution of Eqs. (6), (7), (9) and (11) to obtain the parameter N (Table 1).
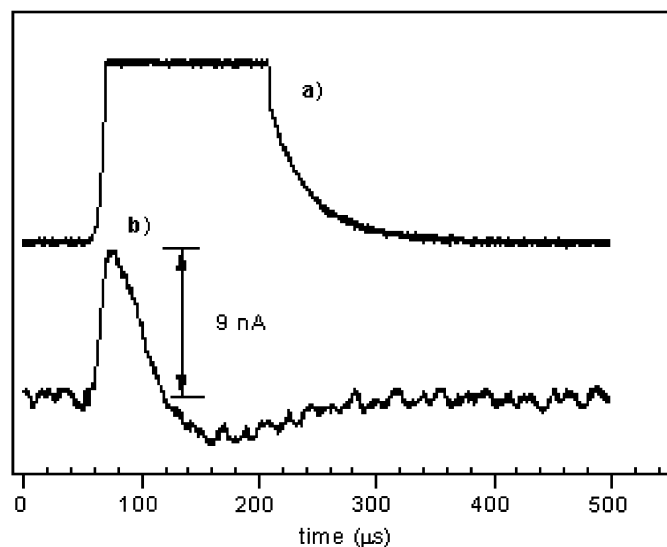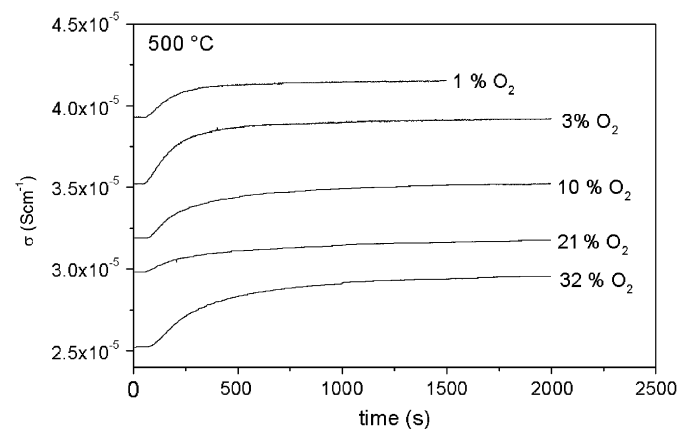

Fig. 2. Dual channel oscilloscope traces of: (a) the photodiode monitored response to a Xe lamp pulse excitation and (b) the induced photocurrent response on a γ'-Bi_2MoO_6 thick film, heated to 235 °C, preamplified to 10^{-8} A/V.

Fig. 3. Temporal dependence of electrical conductivity at 500 °C for γ'-Bi_2MoO_6 at controlled partial pressures of oxygen.

Between 450 and 550 °C increased conductivity is invariably observed with diminishing p_{O_2} (Fig. 4a), which is consistent with a minimum total conductivity corresponding to a stoichiometric phase, for the positive pressure range not accessible with the ceramic reaction vessels employed in this work. At low vacancy concentration, the ideal approximation implicit in the derivation of Eqs. (6) and (9) is valid, and N approaches the value 0.16, predicted by Eq. (9) for a simple model of doubly ionized oxygen vacancies (V_O^{++}) and interstitial oxygen (O_i^{2-}) (Table 1, $N2$). Point defect interaction becomes significant under increasingly reducing atmospheres, which attenuates the observed p_{O_2} dependence (Table 1, $N1$).

Above 600 °C, increased Frenkel disorder renders the p_{O_2} dependence of the conductivity neither monotonic nor significant ($N < 0.06$), consistently with $[O_i^{2-}] = [V_O^{++}]$ and dominant ionic conductivity.

Table 1
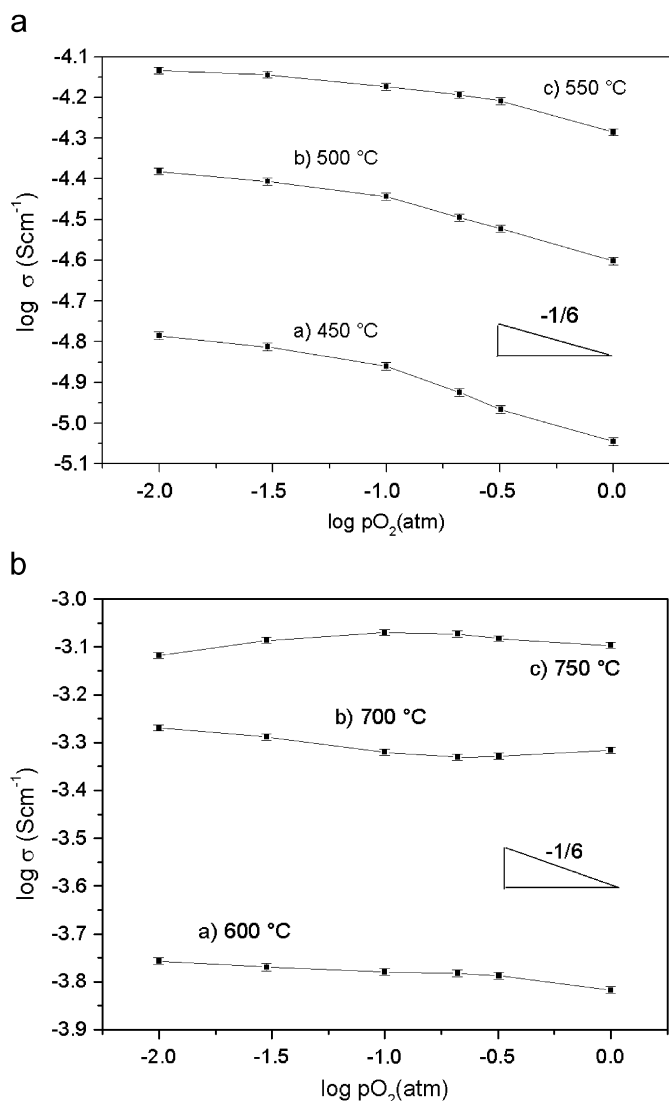N values obtained from fits to Eq. (12) for the data reported in Fig. 4a and b

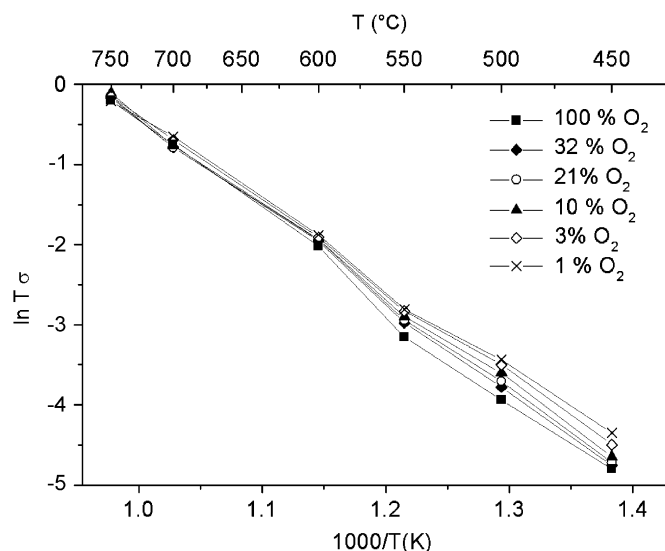| T (°C)	$N1$	$N2$
450	−0.05 (0.03–0.01 atm)	−0.16 (1–0.03 atm)
500	−0.06 (0.1–0.01 atm)	−0.16 (1–0.1 atm)
550	−0.06 (0.32–0.03 atm)	−0.16 (1–0.32 atm)
	−0.02 (0.03–0.01 atm)	
600	−0.06 (1–0.32 atm)	
	−0.02 (0.32–0.01 atm)	
700	0.02 (1–0.21 atm)	
	−0.04 (0.03–0.01 atm)	
750	−0.06 (1–0.1 atm)	
	0.03 (0.1–0.03 atm)	

Fig. 5. Arrhenius plots of the thermal dependence of γ'-Bi$_2$MoO$_6$ conductivity at selected constant partial pressures of oxygen.

The thermal dependence of the extrapolated conductivities (Fig. 5) changes between 550 and 600 °C, in apparent coincidence with the γ'' to γ' transition reported [1,2] at that temperature; however, the observed conductivity change is entirely reversible upon repeated thermal recycling, whereas the γ'' transforms to γ' irreversibly [1]. For total conduction data sampled at fixed frequency, the apparent activation energies of 0.89 eV above and 0.84 eV, below 550 °C, do not pertain to elementary processes and reflect instead the gradual change in dominant carrier type, as well as conduction path [16].

6. Conclusions

γ'-Bi$_2$MoO$_6$ is a mixed ionic–electronic conductor. Electronically conducting layered perovskites of the rare earth transition metal oxides [20,21] provide instances of $+\frac{1}{6}$ power law dependence on oxygen partial pressure, associated with oxygen excess, whereas the $-\frac{1}{6}$ power observed in this study is indicative of oxygen deficiency

Fig. 4. (a) Oxygen partial pressure dependence of the equilibrium electrical conductivity in γ'-Bi$_2$MoO$_6$ at 450, 500 and 550 °C. (b) Oxygen partial pressure dependence of the equilibrium electrical conductivity in γ'-Bi$_2$MoO$_6$ at 600, 700 and 750 °C.

with doubly ionized vacancies. The singular structural feature [1,2] is the presence of tunnels normal to the layers, which mediate fast ionic oxygen transport and ionic conduction overwhelming the electronic contribution above 600 °C; nonetheless, conductivity response to stoichiometric changes is fast and highly reversible with typical responses in the order of minutes, unlike oxides in which lattice oxygen migration requires substantial relaxation times.

References

[1] D.J. Buttrey, T. Vogt, U. Wildgruber, W.R. Robinson, J. Solid State Chem. 111 (1994) 118–127.

[2] D.J. Buttrey, D.A. Jeferson, J.M. Thomas, Philos. Mag. A 53 (1986) 897–906.

[3] D.A.G. van Oeffelen, J.H.C. van Hooff, G.C.A. Schuit, J. Catal. 95 (1985) 84–100.

[4] L.T. Sim, C.K. Lee, A.R. West, J. Mater.Chem. 12 (2002) 17–19.

[5] P. Shuk, H.-D. Wiemhöfer, U. Guth, W. Göpel, M. Greenblatt, Solid State Ionics 89 (1996) 179–196.

[6] A. Ziehfreund, W.F. Maier, Chem. Mater. 8 (1996) 2721–2729.

[7] P.G. Bruce, Solid State Electrochemistry, Cambridge University Press, Cambridge, 1995, 39pp.

[8] J.R. Macdonald, Impedance Spectroscopy, Wiley, New York, 1987.

[9] F.A. Kröger, H.J. Vink, in: F. Seitz, D. Turnbull (Eds.), Solid State Physics, vol. 3, Academic Press, New York, 1956.

[10] R.B. Fair, Sensors Actuators 1 (3) (1981) 305–328.

[11] A.J. Crocker, Sensors Actuators 1 (3) (1981) 347–378.

[12] J.M. Essick, R.T. Mather, Am. J. Phys. 61 (7) (1993) 646–649.

[13] W.W. Wendlandt, H.G. Hecht, Reflectance Spectroscopy, Wiley Interscience, New York, 1966, 298pp.

[14] G. Kottim, Reflectance Spectroscopy, Springer, New York, 1969.

[15] D.T. Stevenson, R.J. Keyes, J. Appl. Phys. 26 (1955) 190.

[16] C.M.C. Vera, R. Aragón, Mater. Sci. Eng. B 121 (2005) 187–191.

[17] I. Riess, Solid State Ionics 91 (1996) 221–232.

[18] I. Riess, Solid State Ionics 157 (2003) 1–17.

[19] C.M.C. Vera, R. Aragón, Rev. Mex. Fís. S 52 (2) (2006) 20–22.

[20] P.A. Salvador, L. Shen, T.O. Mason, K.B. Greenwood, K.R. Poeppelmeier, J. Solid State Chem. 119 (1995) 80–89.

[21] V.V. Kharton, A.A. Yaremchenko, A.L. Shaula, M.V. Patrakeev, E.N. Naumovich, D.I. Logvinovich, J.R. Frade, F.M.B. Marques, J. Solid State Chem. 177 (2004) 26–37.